

SPE 40038

## Application of Conventional Well Logs to Characterize Naturally Fractured Reservoirs with their Hydraulic (Flow) Units; A Novel Approach

Tarek Ibrahim Elkewidy, SPE, GeoRes 4D (Grant Geophysical); and Djebbar Tiab, SPE, University of Oklahoma

Copyright 1998, Society of Petroleum Engineers, Inc.

This paper was prepared for presentation at the SPE Gas Technology Symposium held in Calgary, Canada, 15-18 March, 1998.

This paper was selected for presentation by an SPE Program Committee following review of information contained in an abstract submitted by the author(s). Contents of the paper, as presented, have not been reviewed by the Society of Petroleum Engineers and are subject to correction by the author(s). The material, as presented, does not necessarily reflect any position of the Society of Petroleum Engineers, its officers, or members. Papers presented at SPE meetings are subject to publication review by Editorial Committees of the Society of Petroleum Engineers. Electronic reproduction, distribution, or storage of any part of this paper for commercial purposes without the written consent of the Society of Petroleum Engineers is prohibited. Permission to reproduce in print is restricted to an abstract of not more than 300 words; illustrations may not be copied. The abstract must contain conspicuous acknowledgment of where and by whom the paper was presented. Write Librarian, SPE, P.O. Box 833836, Richardson, TX 75083-3836, U.S.A., fax 01-972-952-9435.

### Abstract

This study introduces a new practical and cost-effective technique to in-situ describes the most important petrophysical properties of naturally fractured reservoirs. Cores from naturally fractured formations may not be representative and thus the analysis are not reliable. Well logging interpretation of porosity and resistivity can provide the required in-situ measurements.

Here, formation total porosity, which may be estimated from conventional wireline logs, and cementation exponent, which can be determined from crossplotting log porosity versus log resistivity are the only two parameters required to uniquely derive resistivity factor, tortuosity, partitioning coefficient, fracture intensity index, matrix porosity, fracture porosity, and fracture storativity ratio for naturally fractured formations at reservoir conditions. Furthermore, these well log derived parameters are utilized along with correlated core data to express Reservoir Quality Index (RQI) in terms of partitioning coefficient and fracture intensity index. This RQI may be, then, used to characterize the different hydraulic (flow) units of naturally fractured reservoirs.

The product of this novel approach is an easy, flexible, and cost effective method that is readily adaptable to different naturally fractured formations including clastics, carbonates, and basement. This study will present the theory, application example, and practical charts for estimating the various rock properties. Application of this technique may ultimately result in opening new potentials, particularly in carbonates, redrilling or reentering hydrocarbon bearing intervals that were bypassed.

### Introduction

Naturally fractured reservoirs may be composed of any lithology including clastics (sands or shales), carbonates, and even basement rocks. However, they are more pronounced and attractive in carbonates. Several investigators have attempted to evaluate naturally fractured reservoirs using various methods ranging from the macroscopic scale of core analysis through the mesoscopic scale of well logging up to the megascopic scale of pressure transient analysis and 3-D seismic. Each of those methods has certain advantages, limitations, applicability and reliability.<sup>1</sup>

The key to unlock the hydrocarbon potential of a naturally fractured reservoir is to evaluate its static hydrocarbon content through accurate determination of water saturation, and predict its dynamic flow capacity through estimation of porosity and permeability. This characterization should be performed both in the matrix and the fractures systems at the reservoir native conditions.

More emphasis is aimed in this study upon generating an innovative method to characterize the various petrophysical properties of naturally fractured reservoirs from conventional well logging techniques. Generally, well logs provide in-situ measurements compared to core analysis and posses higher resolution compared to well testing techniques. Here, conventional well log measurements of formation resistivity-porosity and evaluation concepts of crossplots, bulk volume water, partitioning coefficient, and fracture intensity index provide the tools for the novel technique. The proposed technique is quite simple. It is based upon deriving formation resistivity factor, tortuosity, partitioning coefficient, fracture intensity index, matrix porosity, fracture porosity, and fracture storativity ratio for naturally fractured formations at reservoir conditions in terms of total porosity,  $\phi_t$ , and cementation exponent,  $m$ , only.

The technique is further extended to characterize the various hydraulic (flow) units in heterogeneous naturally fractured reservoirs. A hydraulic unit may be defined as "a continuous body over a specific reservoir volume that practically possesses consistent petrophysical and fluid properties, which uniquely characterize its static and dynamic state distinguishing it from other rock volumes."<sup>1</sup> The concept

of reservoir quality index and its attributes are adapted to characterize naturally fractured flow units utilizing the new technique.

#### Methods of Evaluating Naturally Fractured Reservoirs.

Fractured reservoirs can be evaluated using three techniques:

1. Core analysis
2. Well logging
3. Pressure transient analysis.

Core analysis of naturally fractured reservoirs is not very reliable. In fact, accurate assessment of porosity in a dual-porosity system (e.g., matrix and fractures) is critical for estimating in-place reserves and producibility of the formation. However, the magnitude range of fracture porosity and consequently its contribution to the total reservoir fluid capacity is still a matter of controversy among researchers.<sup>1</sup> The void volume of a fractured formation is a function of the fracture frequency and clearance (width) within the investigated rock block. Several investigators reported various ranges of fracture porosity.<sup>2</sup> This discrepancy is a natural result of using different methods for estimating fracture porosity,  $\phi_f$ , from core analysis and of how representative the core plug is to the real reservoir. Table 1 shows the results of a literature survey updated after Hensel Jr. (1989)<sup>2</sup> on fracture width and frequency from different formations as reported by various authors. Very little is documented regarding fracture frequency. Determination of fracture dimension and porosity in the laboratory is not reliable because cores, which contain fractures of practical significance, are often lost in the process of recovery. Furthermore, some fractures form during the recovery process of cores as a result of coring and stress release.

Table 2 lists the results of fracture porosity determined by laboratory measurements on different core samples from different formations as reported. Notice the wide range of fracture porosity 0.001-9.64%. Actually, fracture studies from core analysis could be misleading, especially if not enough samples are available through the reservoir. There will always be the question, in the kind of heterogeneous formations, of how representative the core samples are to the real fracture distribution within the reservoir. A full size core may be more reliable in this case. Another major factor in fracture distribution is that they tend to be more associated and intense near formation structures (faults and folds).

Fractured reservoirs can be also characterized using well logging techniques. Several methods are available to detect natural and induced fractures in the reservoir from well log data.<sup>3</sup> Well logging have the advantages of furnishing more coverage of the formation within the well as well as across the reservoir and providing in-situ measurements of the formation at reservoir conditions. Fracture effects on porosity are in-situ reflected on the measured total porosity from neutron and density tools. The effect is also reflected on the cementation exponent,  $m$ , of Archie's equation as will be discussed in the following section.

For example, Fig. 1 is for a well from the Gulf Coast. In

this well, gamma ray and induction logs were run at three different times. In run A, gamma ray and induction logs were conducted following drilling with 17.1 lb/gal inverted oil emulsion mud. As the well was deepened to 16,294 ft, a pressure kick occurred. Consequently, the mud density was increased to 17.5 lb/gal. Mud and mud filtrate invaded the formation, losing 275 bbls of mud. Run B was, then, conducted nine days after run A. Later on, mud density was decreased to 17.3 lb/gal. An increase in the mud volume was noticed. Comparing run B with run A indicates a general increase in formation resistivity,  $R_{IL}$ , especially between 15,910 and 15,925 ft. The general increase in  $R_{IL}$ , can be interpreted as an increase in the depth of invasion by the nonconductive mud filtrate. Whereas, the formation was fractured at those higher resistivity readings as a result of increasing mud weight from 17.1 to 17.5 lb/gal. Most of the 275 bbls were placed in the induced fractures, which are imprinted as high resistivity kicks on the log. When the mud weight was reduced to 17.3 lb/gal most of the mud in the induced fractures flowed back to the well as indicated by the lower resistivity reading of run C.<sup>3</sup>

Pressure transient analysis methods have several applications in evaluating naturally fractured reservoirs. However, the characterization in this case is averaged over the megascopic scale of the interwell spacing or the whole formation that is in hydraulic communication with the well. Therefore, well logging techniques are good candidates for characterizing naturally fractured reservoirs since they provide in-situ measurements compared to core analysis and possess higher resolution compared to well testing. It should be stressed that, a combination of well logging and core analysis techniques (particularly from full size core) is very valuable especially for exploration purposes. An integrated cross-correlation approach between the three scales of characterizations to confirm the evaluation may optimize the process.

#### Cementation Exponent, $m$ , in Naturally Fractured Reservoirs.

Cementation exponent,  $m$ , is one of the important variables in Archie's equation which is considered to be the fundamental of formation evaluation from well logs. Archie's equation is given in general terms as

$$S_w^n = \frac{aR_w}{\phi^m R_t} \quad \dots \dots \dots (1)$$

Usually the value of  $m$  is assumed equal to 2.0 for formations with interparticle (grains or crystals) porosity. Theoretically, the value of  $m$  for a plane fracture equals 1.0. This can be proven by considering the following relationships between formation resistivity factor,  $F$ , tortuosity,  $\tau$ , porosity,  $\phi$ , and cementation exponent,  $m$ :

$$F = \frac{R_o}{R_w} = \frac{\tau}{\phi} \quad \dots \dots \dots (2)$$

$$F = \frac{1}{\phi^m} \dots\dots\dots (3)$$

Since, tortuosity for a plane straight fracture equals 1.0, then combining Eqs. 2 and 3 suggests that  $m=1.0$  for a plane fracture. Some researchers have proposed different relationships between  $F$  and  $\tau$  depending on the model used to simulate the porous medium.<sup>4,5</sup> However, the correlation of Eq. 2 will be used consistently in this study since it is based on a more realistic representation of the reservoir rock by considering the average cross-sectional area open to flow.<sup>3</sup> In Eq. 3, coefficient "a" is assigned a value of 1.0. A recent study by Maute, R. E. et al. (1992) recommended a fixed value of  $a = 1.0$ , and concluded that there is no practical difference in water saturation error between a fixed and variable "a" values.<sup>6</sup> Actually, the original Archie's equation does not include parameter "a."

In reality, fractures are not plane. They usually have a more or less tortuous path, so naturally fractured reservoirs will exhibit a value for the cementation exponent,  $m$ , in the range between 1.0 and 2.0 depending on the intensity of fracturing and the interaction between fracture voids and matrix voids. Furthermore, a naturally fractured formation may have a value of  $m$  slightly higher than 2.0 if it contains shaly material. The tortuosity of formations with shaly contents is greater than that of shale free formations. Cementation exponent,  $m$ , increases with the degree of shaleness in the reservoir.<sup>7</sup> Interrelated factors influencing cementation exponent,  $m$ , can be summarized as:<sup>1,8</sup>

1. Pore-pore throat geometry which reflects
  - a) Tortuosity
  - b) Specific surface area
  - c) Grain shape
  - d) Cementation
  - e) Uniformity of mineral mixture distribution
  - f) Clay content and distribution
2. Anisotropy
3. Degree of electrical isolation
4. The occurrence of open fractures

Accurate determination of  $m$  value is critical for estimating the hydrocarbon reserve. Fig. 2 illustrates the magnitude of error in hydrocarbon reserve that may result due to the usual assumption of  $m = 2.0$  while the true value of  $m$  is other than 2.0. The error in reserve estimate for the case of  $n = 2.0$  is given by:

$$\text{error in reserve estimate} = \frac{100(1 - \phi^{1-0.5m})}{\phi^{1-0.5m}} \dots\dots\dots (4)$$

Notice that the highest error occurs at low porosity which is the usual case with naturally fractured reservoirs. Many researchers have proposed various empirical formulas to determine cementation exponent,  $m$  from log measurements.<sup>8,9</sup> Each of these formulas is applicable only to certain pore geometry and/or formation kind provided that porosity type is

known in advance. Significant differences in the calculated  $m$  value may result by using the incorrect formula. For example, a formation with water resistivity  $R_w = 0.04$  ohm-m, true formation resistivity  $R_t = 20.0$  ohm-m, sonic porosity  $\phi = 0.05$  may be assigned a cementation exponent  $m = 3.16$  calculated using Nugent (1984) formula if a vuggy porosity is assumed. This will result in a calculated water saturation  $S_w = 89.6\%$ . Whereas, if fracture plus vuggy porosity is assumed then the calculated  $m$  value using Rasmus (1983) formula will be 1.20. In contrast this will indicate a hydrocarbon-bearing reservoir with calculated water saturation,  $S_w$ , of only 13.9%.<sup>8</sup>

An alternative, universal, and more accurate approach to calculate  $m$  and characterize hydraulic units within reservoirs that have different and/or heterogeneous pore-pore throat geometry including naturally fractured reservoirs is by constructing a log porosity versus log resistivity crossplot (Pickett plot). Observations indicate that this crossplotting technique can be a very powerful, flexible, practical and cost effective tool to characterize different kinds of reservoirs including those with shaly contents.<sup>1</sup> It should be noted that a relatively wide range of porosity and resistivity data is needed to construct such a crossplot. However, even with few data, reliable information can be extracted from the technique with good engineering and geological judgements.<sup>1,5</sup> The well log derived porosity has to reflect the total formation porosity which include the matrix (primary) and the vuggy/fracture (secondary) porosities. Porosity derived from density-neutron crossplot will serve the purpose. The crossplotting technique will be elaborated upon more within the application example.

Two main concepts are usually used to characterize naturally fractured reservoirs; the concept of partitioning coefficient,  $v$ , and the concept of fracture intensity index, FII.

**Concept of Partitioning Coefficient,  $v$ .**

Partitioning coefficient,  $v$ , simply represents the apportioning of total porosity,  $\phi_t$ , between interparticle (matrix) porosity,  $\phi_{ma}$  and the larger pores (vugs, fissures, fractures,  $\phi_f$ , etc.). It is usually given by:<sup>3,15</sup>

$$v = \frac{\phi_t - \phi_{ma}}{\phi_t(1 - \phi_{ma})} \dots\dots\dots (5)$$

**Concept of Fracture Intensity Index, FII.**

Pirson (1967) introduced the concept of Fracture Intensity index, FII. It represents the magnitude of formation porosity attributed to fractures as the ratio between secondary porosity (fractures) to the solid rock volume as:<sup>14</sup>

$$FII = \frac{\phi_t - \phi_{ma}}{1 - \phi_{ma}} \dots\dots\dots (6)$$

Thus, FII is related to the partitioning coefficient,  $v$ , by:

$$FII = v\varphi_t \quad \dots\dots\dots (7)$$

Fracture intensity index can be determined from core analysis (e.g., Lock-Bliss method), well logging evaluation, or pressure transient analysis. However, since core analysis techniques are based on examining a fraction of the reservoir (core plug) which may not accurately represent the extent of fractures in the formation, an in-situ determination of FII using either well logging or pressure transient evaluations is more desirable.

When  $v$ , and  $\varphi_t$  are available then the following parameters can be estimated for a naturally fractured reservoir:

$$\varphi_f = \frac{FII(\varphi_t - 1)}{v\varphi_t - 1} \quad \dots\dots\dots (8)$$

and

$$\varphi_{ma} = \frac{\varphi_t(v - 1)}{v\varphi_t - 1} = \frac{FII - \varphi_t}{FII - 1} \quad \dots\dots\dots (9)$$

Pirson<sup>11-16</sup> considered this double porosity system as two electric circuits, representing the fractures and the matrix porosity, connected in parallel. For a hydrocarbon-bearing formation invaded by electrically conductive mud filtrate Pirson's expressions for formation resistivity can be written in terms of the spherically focused,  $R_{SFL}$ , and the dual induction resistivity logs as:<sup>11</sup>

$$\frac{1}{R_{SFL}} = \frac{v\varphi_t S_{xo}}{R_{mf}} + \frac{(1-v)S_{wma}^2}{R_{mas}} \quad \dots\dots\dots (10)$$

$$\frac{1}{R_{ID}} = \frac{v\varphi_t S_{wf}}{R_w} + \frac{(1-v)S_{wma}^2}{R_{mas}} \quad \dots\dots\dots (11)$$

Eq. 10 postulates that a mud filtrate having a resistivity of  $R_{mf}$  will preferentially invade fractures and vugs with little if any, invasion to the matrix voids. Eqs. 10 and 11 may be also expressed in terms of the recently developed Phasor Induction Resistivity logs,  $R_{IDPH}$ . In the above formulation, mud filtrate depth of invasion has to be shallow in order not to affect the deep induction resistivity. So that, a distinct separation must be observed between the shallow and deep resistivity readings.

For a 100% water saturated formation, where  $S_{xo} = S_{wf} = S_{wma}$ , the two equations can be combined and expressed in terms of the resistivity of the invaded zone,  $R_{xo}$ , and the true formation resistivity,  $R_t$ , to yield:

$$FII = \frac{\frac{1}{R_{xo}} - \frac{1}{R_t}}{\frac{1}{R_{mf}} - \frac{1}{R_w}} \quad \dots\dots\dots (12)$$

where  $R_{xo}$  and  $R_t$  are derived from  $R_{SFL}$  and  $R_{ID}$ , respectively, after correction for logging environment and depth of mud filtrate invasion.

#### Determination of Partitioning Coefficient and Fracture Intensity Index from Well Log Data (A Novel Technique).

For a double porosity fractured reservoir with 100% formation water saturation, Eq. 11 can be written as:

$$\frac{1}{R_o} = \frac{v\varphi_t}{R_w} + \frac{1-v}{R_{mas}} \quad \dots\dots\dots (13)$$

where  $R_{mas}$  is the resistivity of 100% water saturated matrix and  $R_o$  is the resistivity of the total system (matrix voids + fracture voids), 100% water saturated. Aguillera (1995) rearranged Eq. 13 to:<sup>3</sup>

$$R_o = \frac{R_w R_{mas}}{v\varphi_t R_{mas} + (1-v)R_w} \quad \dots\dots\dots (14)$$

Substituting Eq. 2 into 14 yields:

$$F = \frac{R_{mas}}{v\varphi_t R_{mas} + (1-v)R_w} \quad \dots\dots\dots (15)$$

Aguillera considered a cementation exponent,  $m$ , for the whole matrix-fracture system and another exponent,  $m_b$ , for the matrix alone where  $m < m_b$ . Then, Eq. 15 was rewritten as:

$$\varphi_t^{-m} = \frac{1}{v\varphi_t + \frac{(1-v)}{\varphi_{ma}^{-m_b}}} \quad \dots\dots\dots (16)$$

Utilizing Eq. 13, Aguillera developed charts to estimate  $\varphi_t$ ,  $\varphi_{ma}$ ,  $m$  and  $v$ .<sup>3</sup> However, to use these charts a value for  $m_b$  has to be determined from precise core analysis or (as usual) assumed. Actually, there is no need to differentiate between  $m$  and  $m_b$  when evaluating fractured reservoirs using well logs. Well logs will sense only one effective cementation exponent,  $m$ , (according to Archie's law) reflecting the effective system tortuosity among other factors including shale effect. This effective cementation exponent can be accurately determined using log  $\varphi_t$  versus log  $R_t$  crossplot technique.

Introducing a practical technique to determine fractures

partitioning coefficient,  $\nu$ , from well log data as follows:  
 Since

$$F = \frac{1}{\phi_t^m} \dots\dots\dots (17)$$

then substituting into Eq. 15 results in

$$\frac{1}{\phi_t^m} = \frac{R_{mas}}{\nu\phi_t R_{mas} + (1-\nu)R_w} \dots\dots\dots (18)$$

Rearranging and solving for  $\nu$ , then

$$\nu = \frac{\phi_t^m R_{mas} - R_w}{\phi_t R_{mas} - R_w} \dots\dots\dots (19)$$

Neglecting  $R_w$  from Eq. 19 (since  $R_{mas} \gg R_w$ ) then,  $\nu$  can be expressed by the following simple formula with practically minimal error averaging about 3 % (decreases with increasing fracture intensity)

$$\nu = \phi_t^{m-1} \dots\dots\dots (20)$$

Partitioning coefficients calculated using Eq. 20 is in very good agreement with those estimated from Aguilera's charts if the matrix cementation exponent  $m_b$  is known. Eq. 20 represents a breakthrough in formation evaluation of naturally fractured reservoirs. It opens a new dimension for the relationships between FII,  $F$ ,  $\tau$ ,  $\phi_t$  and  $m$  for fractured formations since the first three variables can be expressed as:

Fracture Intensity Index, FII

$$FII = \phi_t^m \dots\dots\dots (21)$$

Formation resistivity factor,  $F$

$$F = \phi_t^{-m} \dots\dots\dots (22)$$

Formation tortuosity,  $\tau$

$$\tau = \phi_t^{1-m} \dots\dots\dots (23)$$

Figs. 3 and 4 illustrate practical charts to determine  $F$  and  $\tau$  while Figs. 5 and 6 show other charts to determine  $\nu$  and FII for different values of  $\phi_t$  and  $m$ .

Furthermore, accurate assessment of porosity in a dual-porosity system (e.g., matrix and fractures) is critical for estimating in-place reserves and producibility of the formation. However, the range of magnitude of fracture

porosity and consequently its contribution to the total reservoir fluid capacity is still a matter of controversy among researchers as previously explained.

Now, Eqs. 8 and 9 can be effectively simplified to yield fracture porosity,  $\phi_f$ , and matrix porosity,  $\phi_{ma}$ , in terms of  $\phi_t$  and  $m$  only as:

$$\phi_f = \frac{\phi_t^{m+1} - \phi_t^m}{\phi_t^m - 1} \dots\dots\dots (24)$$

and

$$\phi_{ma} = \frac{\phi_t^m - \phi_t}{\phi_t^m - 1} \dots\dots\dots (25)$$

Eqs. 24 and 25 provide accurate in-situ determination of  $\phi_f$  and  $\phi_{ma}$  on a wider range within wells drilled throughout the reservoir. For example, a fractured formation that has a total porosity of 10% and an effective cementation exponent of 1.85, Eq. 24 yields a fractured porosity of 1.29%, whereas Eq. 25 yields a matrix porosity of 8.71%. Figs. 7 and 8 illustrate practical charts to determine  $\phi_f$  and  $\phi_m$  for fractured reservoirs knowing  $\phi_t$  and  $m$ . The concern of accounting for fractures which tend to be more intense near structures that could be away from the well may be resolved by estimating  $\nu$ , FII, and even  $m$  from pressure transient analysis.<sup>17</sup>

So, with knowledge of  $\phi_t$  and  $m$  (as determined from log  $\phi_t$  versus log  $R_t$  crossplot) all the above mentioned dimensionless parameters can be evaluated to universally characterize naturally fractured reservoirs. In addition cementation exponent,  $m$ , may be determined from any of the above equations, when the corresponding parameter is available through other sources, e.g.

$$m = \frac{\log \nu}{\log \phi_t} + 1 \dots\dots\dots (26)$$

Moreover, several combinations of relationships can be established among parameters,  $F$ ,  $\tau$ ,  $\nu$ , FII, and expressed in terms of resistivity, e.g.

$$\tau = \phi_t F = \frac{\phi_t R_o}{R_w} = \frac{\phi_t R_{xos}}{R_{mf}} \dots\dots\dots (27)$$

$$\nu = \frac{1}{\phi_t F} = \frac{R_w}{\phi_t R_o} = \frac{R_{mf}}{\phi_t R_{xos}} \dots\dots\dots (28)$$

$$FII = \frac{1}{F} = \frac{R_w}{R_o} = \frac{R_{mf}}{R_{xos}} \dots\dots\dots (29)$$

also

$$v = \frac{1}{\tau} \dots\dots\dots (30)$$

$$FII = \frac{\phi_t}{\tau} \dots\dots\dots (31)$$

where  $R_{xo}$  is the resistivity of the invaded zone, 100% saturated with conductive mud filtrate.

Partitioning coefficient,  $v$ , may be also estimated in oil-bearing formation by rewriting Eq. 11 in the form of:

$$\frac{1}{R_t} = \frac{v\phi_t S_{wf}}{R_w} + \frac{(1-v)S_{wma}^2}{R_{mas}} \dots\dots\dots (32)$$

where  $S_{wf}$  is water saturation in the fracture voids and  $S_{wma}$  is water saturation in the matrix voids. Resistivity of the matrix can be evaluated from the deep induction log in front of an unfractured portion of the reservoir or may be approximated by  $\phi_{ma}^{-2}R_w$  where  $\phi_{ma}$  is to be obtained from acoustic porosity log, consequently  $S_{wma}$ .

Another important property of naturally fractured reservoirs, often derived from pressure transient analysis, is the fracture storativity ratio,  $\omega$ . It estimates the ratio of oil production from the fractures system to the total oil production from both the fractures and the matrix in under saturated reservoirs. Using the new technique of expressing fracture porosity and matrix porosity in terms of total porosity and cementation exponent, fracture storativity ratio can be simply expressed as:

$$\omega = \frac{\phi_t^m - \phi_t^{m-1}}{\phi_t^m - 1} \dots\dots\dots (33)$$

For example, a naturally fractured reservoir with a total porosity of 10% and an effective cementation exponent of 1.85 will have a storativity ratio of 12.89%. Fig. 9 illustrates a practical chart to estimate  $\omega$  from knowledge of  $\phi_t$  and  $m$ .

It is interesting to note that Jorgensen (1988) developed a model to estimate formation permeability as a function of total porosity and cementation exponent as:<sup>18</sup>

$$K = 84105 \frac{\phi^{m+2}}{(1-\phi)} \dots\dots\dots (34)$$

**Calculating Partitioning Coefficient and Fracture Intensity Index for Formations Drilled with Nonconductive Mud.**

Fracture intensity index given in terms of well logging parameters by Eq. 12 is valid only for 100% water saturated zones drilled with a water-base mud that yields conductive brine filtrate. For the case of drilling with oil-base mud yielding nonconductive mud filtrate Eqs. 10 and 11 can be

rewritten taken into account the presence of hydrocarbon in the system as:

$$\frac{1}{R_{xo}} = \frac{v\phi_t S_{xo}}{R_w} + \frac{(1-v)S_w^2}{R_{mas}} \dots\dots\dots (35)$$

$$\frac{1}{R_t} = \frac{v\phi_t S_w}{R_w} + \frac{(1-v)S_w^2}{R_{mas}} \dots\dots\dots (36)$$

In Eq. 35  $R_w$  has replaced  $R_{mf}$  since in the case of oil-base mud filtrate, formation water is the only electrolyte present in both the invaded and the virgin zones. Also, water saturation in the uninvaded fracture system is considered equal to that in the matrix, i.e.,  $S_{wf} = S_{ma} = S_w$ .

Subtracting Eq. 35 from 36 results in an expression for FII, in this case of oil-base mud filtrate invasion, as:

$$FII = \frac{R_w \left( \frac{1}{R_t} - \frac{1}{R_{xo}} \right)}{S_w - S_{xo}} \dots\dots\dots (37)$$

A new method to calculate the correct  $R_t$ ,  $R_{xo}$ ,  $S_w$ , and  $S_{xo}$  in formations drilled with oil-base mud is explained in reference 19. Once the correct  $\phi_t$  and  $R_t$  have been determined, the concept of crossplotting  $\log \phi_t$  versus  $\log R_t$  can be implemented to extract the correct cementation exponent,  $m$ . Then, the system of Eqs. 20 through 25 in addition to 33 can be evaluated in this case of drilling with nonconductive mud.

**Extension of Reservoir Quality Index Concept to Naturally Fractured Reservoirs.**

The concept of Reservoir Quality Index, RQI, was discussed in details by Amaefule et al. (1993)<sup>20</sup> as a tool to aid the process of characterizing the formation into its different hydraulic (flow) units. RQI, which was driven from a generalized form of Kozeny-Carmen correlation can be written in the form of:

$$RQI = 0.0314 \sqrt{\frac{k}{\phi}} = \left( \frac{1}{\tau \sqrt{F_s} \gamma S_{gv}} \right) \left( \frac{\phi}{1-\phi} \right) \dots\dots\dots (38)$$

where RQI is in micrometers, permeability in milli-darcy, and porosity in fraction. The fraction of the pore space that is water wet,  $\gamma$ , is introduced to the above formulation in order to account for the effect of wettability.<sup>1</sup>

This concept and its attributes was introduced essentially for shale free clastic reservoirs with interparticle porosity.<sup>20,21</sup> It can be extended to formations with natural fractures by expressing the effective zoning factor,  $Z_e$ , hydraulic unit characterization factor,  $H_c$ , flow zone indicator, FZI, and

average permeability,  $K$ , in terms of either partitioning coefficient,  $v$ , fracture intensity index,  $FII$ , or cementation exponent,  $m$ , and total porosity,  $\phi_t$  as follows:

$$Z_c = F_s \tau^2 = F_s \phi_t^{2(1-m)} = \frac{F_s}{v^2} = \frac{F_s \phi_t^2}{FII^2} \dots\dots\dots (39)$$

$$H_c = Z_c S_{gv}^2 = F_s \phi_t^{2(1-m)} S_{gv}^2 = \frac{F_s}{v^2} S_{gv}^2 = \frac{F_s \phi_t^2}{FII^2} S_{gv}^2$$

$$= F_s S_{pv}^2 \frac{\phi^{4-2m}}{(1-\phi_t)^2} \dots\dots\dots (40)$$

$$FZI = \frac{1}{\sqrt{H_c}} = \frac{1}{\phi_t^{(1-m)} \sqrt{F_s S_{gv}}} = \frac{v}{\sqrt{F_s S_{gv}}} = \frac{FII}{\phi_t \sqrt{F_s S_{gv}}} = \frac{1-\phi_t}{\sqrt{F_s S_{pv}} \phi_t^{2-m}} \dots\dots\dots (41)$$

$$K = FZI^2 \frac{\phi_t^3}{(1-\phi_t)^2} = \frac{1}{F_s S_{gv}^2} \frac{\phi_t^{2m+1}}{(1-\phi_t)^2} = \frac{v^2}{F_s S_{gv}^2} \frac{\phi_t^3}{(1-\phi_t)^2}$$

$$= \frac{FII^2}{\phi_t^2 F_s S_{gv}^2} \frac{\phi_t^3}{(1-\phi_t)^2} = \frac{\phi_t^{2m-1}}{F_s S_{pv}^2} \dots\dots\dots (42)$$

Then

$$RQI = 0.0134 \sqrt{\frac{K}{\phi_t}} = \frac{1}{\sqrt{F_s S_{gv}}} \frac{\phi_t^m}{(1-\phi_t)}$$

$$= \frac{v}{\sqrt{F_s S_{gv}}} \frac{\phi_t}{(1-\phi_t)} = \frac{FII}{\sqrt{F_s S_{gv}}} \frac{1}{(1-\phi_t)} = \frac{\phi_t^{m-1}}{\sqrt{F_s S_{pv}}} \dots\dots\dots (43)$$

Eqs. 39 through 43 may also be expressed in terms of resistivity by substituting from Eqs. 27 through 29, e.g.

$$RQI = 0.0134 \sqrt{\frac{K}{\phi_t}} = \frac{1}{F \sqrt{F_s S_{gv}}} \frac{1}{(1-\phi_t)}$$

$$= \frac{R_w}{R_o \sqrt{F_s S_{gv}}} \frac{1}{(1-\phi_t)} = \frac{R_{mf}}{R_{xos} \sqrt{F_s S_{gv}}} \frac{1}{(1-\phi_t)}$$

$$= \frac{1}{F \sqrt{F_s S_{pv}} \phi_t} \dots\dots\dots (44)$$

Parameters such as  $F_s$ ,  $S_{gv}$ , and  $S_{pv}$  need to be evaluated from correlated core data. For more information about characterization of hydraulic (flow) units, refer to reference 1 and 20.

**Application Example.**

As indicated before, crossplotting log porosity versus log resistivity is the best technique to in-situ determine the value of cementation exponent,  $m$ , for naturally fractured reservoirs provided that enough data is available. Fig. 10 shows a simulated example of naturally fractured reservoir. The crossplot is constructed based on a general application of Archie's equation in the form of

$$\text{Log} \left( \frac{R_t}{A_{sh}} \right) = \log aR_w - m \log \phi \dots\dots\dots (45)$$

and the concept of irreducible bulk volume water given by

$$BVW_i = S_w \phi = C = \text{constant} \dots\dots\dots (46)$$

to yield:

$$\text{log} \left( \frac{R_t}{A_{sh}} \right)_{irr} = \text{log} \left( \frac{aR_w}{C^n} \right) + (n-m) \log \phi \dots\dots\dots (47)$$

Both Eqs. 45 and 47 resulted in two straight lines on the crossplot with slopes of  $-1/m$  (line FE) and  $1/(n-m)$  (line GE) respectively. So, values for cementation exponent,  $m$ , and saturation exponent,  $n$ , along with  $C$  (point L) and  $aR_w$  (point F) can be all determined for naturally fractured reservoirs at formation conditions provided that the reservoir has zones at 100%  $S_w$  and  $S_{wi}$ .  $A_{sh}$  in Eqs. 45 and 47 is a group of parameters related to the type of shale contents present in the formation if any.<sup>10</sup> For shale free formation  $A_{sh} = 1.0$ . In Fig. 9, the resulting triangle EFG is a unique characteristic indicator for a specific naturally fractured hydraulic unit with essentially constant petrophysical properties.

Crossplotting total porosity versus true resistivity on the log-log scale resulted in the following:

- cementation exponent  $m = 1.85$
- saturation exponent  $n = 1.57$
- $BVW_i$  or  $C = 4.5$  (point E read on the porosity scale)

Other petrophysical parameter are calculated in terms of  $\phi_t$  and  $m$  only and listed in Table 3.

**Conclusions**

1. Petrophysical properties of naturally fractured reservoirs can be evaluated at reservoir conditions from conventional well logging techniques.
2. Formation total porosity and cementation exponent are two important parameters that can be used to uniquely derive formation resistivity factor, tortuosity, partitioning coefficient, fracture intensity index, matrix porosity, fracture porosity, and storativity ratio for naturally fractured.
3. Naturally fractured hydraulic (flow) units can be characterized by expressing RQI concept and its attributes

in terms of the new technique.

4. The product of this novel approach is an easy, flexible, universal, and cost effective technique that is readily adaptable to different naturally fractured formations including clastics, carbonates, and basement.
5. Application of this simple technique may ultimately result in opening new potentials, particularly in uncured carbonates, redrilling or re-entering hydrocarbon-bearing intervals that were by-passed.

### Nomenclature

- a = coefficient related to tortuosity  
 $A_{sh}$  = shale group  
 $BVW_i$  = irreducible bulk volume water  
 C = constant of irreducible bulk volume  
 F = resistivity factor  
 $F_s$  = effective pore throat shape factor  
 FII = fracture intensity index  
 FZI = flow zone indicator  
 $H_c$  = hydraulic unit characterization factor  
 K = average permeability  
 m = cementation exponent  
 $m_b$  = cementation exponent of the matrix  
 n = saturation exponent  
 $R_{ID}$  = deep induction resistivity  
 $R_{mas}$  = resistivity of the matrix, 100% saturated with water  
 $R_{mf}$  = mud filtrate resistivity  
 $R_o$  = formation resistivity, 100 % water saturated  
 RQI = reservoir quality index  
 $R_{SFL}$  = Resistivity from the spherically focused log  
 $R_t$  = true formation resistivity  
 $R_w$  = formation water resistivity  
 $R_{xo}$  = resistivity of the invaded zone  
 $R_{xos}$  = resistivity of the invaded zone, 100% saturated with conductive mud filtrate  
 $S_{gv}$  = specific surface area per unit grain volume  
 $S_{pv}$  = specific internal surface area per unit pore volume  
 $S_w$  = water saturation  
 $S_{wf}$  = water saturation in the fractures system  
 $S_{wma}$  = water saturation in the matrix voids  
 $S_{xo}$  = water saturation in the invaded zone  
 $Z_e$  = effective zoning factor
- $\left(\frac{R_t}{A_{sh}}\right)_{ir}$  = irreducible resistivity group
- $\phi$  = porosity  
 $\phi_f$  = fracture porosity  
 $\phi_{ma}$  = matrix porosity  
 $\phi_t$  = total porosity  
 v = partitioning coefficient  
 $\tau$  = tortuosity  
 $\gamma$  = fraction of the pore spaces that is water wet  
 $\omega$  = storativity ratio

### References

1. Elkewidy, Tarek I.: Characterization of Hydraulic (Flow) Units in Heterogeneous Clastic and Carbonate Reservoirs, a Ph.D. Dissertation, The University of Oklahoma, Norman, Oklahoma, 1996.
2. Hensel, W. M., Jr.: "A Perspective Look at Fracture Porosity," *SPE Formation Evaluation*, December, 1989.
3. Aguilea, R.: *Naturally Fractured Reservoirs*, PennWell Publishing Company, Tulsa, 1995.
4. Cornell, D. and Katz, D. L.: "Flow of Gases Through Consolidated Porous Media," *Ind. Eng. Chem.* (1953), vol. 45, no. 101, p. 2145-2152.
5. Bassiouni, Z.: *Theory, Measurement, and Interpretation of Well Logs*, SPE Textbook Series Vol. 4, Richardson, 1994.
6. Maute, R. E. Lyle, W. D., and Sprunt, E. S.: "Improved Data Analysis Method Determines Archie Parameters from Core Data," *JPT*, January, 1993, p. 103-107.
7. Clavier, C., Coates, G. R., and Dumanoir, J. L.: "Theoretical and Experimental Bases for the Dual-Water Model for the Interpretation of Shaly Sand," *SPEJ*, April, 1984, p. 153-168.
8. Asquith, G. B.: *Handbook of Log Evaluation Techniques for Carbonate Reservoirs*, Methods in Exploration Series No. 5, AAPG, Tulsa, 1984.
9. Wang, F. P. and Lucia, F. J.: "Comparison of Empirical Models for Calculating the Vuggy Porosity and Cementation Exponent of Carbonates from Log Responses," Bureau of Economic Geology, The University of Texas at Austin, 1993.
10. Elkewidy, Tarek I. and Tiab, D.: "Characterization of Hydraulic (Flow) Units in Reservoirs with Shaly Contents," paper SPE 38080, 1997.
11. Pirson, S. J.: "Formation Evaluation by Well Log Interpretation, Part 4," *World Oil*, June, 1957.
12. Pirson, S. J.: *Geologic Well Log Analysis*, Gulf Publishing Company, 1983.
13. Pirson, S. J., et al.: "Fracture Intensity Mapping from Well Logs and from Structure Maps," SPWLA Symposium, paper B, Denver, June, 1967.
14. Pirson, S. J.: "How to Map Fracture Development from Wells Logs," *World Oil*, 1624, no. 4, March 1967, P. 106-114.
15. Pirson, S. J.: "Comprehensive quantitative Well Log Interpretation in Multiple-Porosity Type Reservoir Rocks," *Handbook of Well Log Analysis*, Englewood Cliffs, New Jersey, Prentice-Hall, Inc., 1963, p. 303-314.
16. Pirson, S. J.: "Log Interpretation in Rocks with Multiple Porosity Types - Water or Oil Wet," *World Oil*, June, 1975, p. 196-198.
17. Elkewidy, Tarek I.: "An Original Technique to Evaluate Naturally Fractured Reservoirs from Pressure Transient Analysis," (pending).
18. Jorgensen, G. D.: "Estimating Permeability in Water-Saturated Formations," *The Log Analyst*, Nov-Dec 1988, p. 401-409.
19. Elkewidy, Tarek I.: "A Practical Technique for Formation Evaluation in Reservoirs Drilled with Non-Conductive Muds," (pending).
20. Amaefule, J. O., Altunbay, M., Tiab, D., Kersey, D. and Keelan, D.: "Enhanced Reservoir Description: Using Core and Log Data to Identify Hydraulic (Flow) Units and Predict Permeability in Uncored Intervals/Wells," paper SPE 26436, 1993.
21. Tiab, D., *Modern Core Analysis, Vol. 1-Theory*, Core Laboratories, Houston, Texas, 1993.



**Table 1. Fracture Widths and Spacing,  
(Modified after Hensel, Jr., 1989)**

| Reference               | Formation Information     | Fracture Widths (mm)   |         | Fracture Spacing/<br>Frequency Comments |
|-------------------------|---------------------------|------------------------|---------|---|
|                         |                           | Range                  | Average |   |
| Elkins (1953)           | Spraberry sandstone       | 0.33 (maximum)         | 0.051   | Few inches to a few feet                |
| Snow (1968)             | Selected dam sites        | 0.051 to 0.10          | -       | 4 to 14 ft                              |
| Mar'enko (1978)         | General                   | 0.0001 to 10 up to 100 | -       | -                                       |
| Aguilera (1980)         | General statement         | Paper thin, 6+         | -       | -                                       |
|                         | La Paz-Mara field         | 6.53 (maximum)         | -       | -                                       |
| Weber and Bakker (1981) | Small joints              | 0.01 to 0.10           | -       | -                                       |
|                         | Extension fractures       | 0.1 to 1               | 0.2     | -                                       |
|                         | Major extension fractures | 0.2 to 2               | -       | -                                       |
| Chilingarian (1992)     | General                   | 0.0001 to 0.26         | -       | -                                       |
| Confidential study      | Monterey                  | -                      | 0.01    | 3 to 336 fractures/ft                   |

**Table 2. Porosities of Fractured Reservoirs  
(modified after Hensel, Jr., 1989)**

| References                  | Formation Information    | Porosity Percentage |
|-----------------------------|--------------------------|---------------------|
| Snow (1968)                 | Beaver gas field         | 0.05 to 5           |
| Tkhostove et al. (1970)     | General                  | 0.15 to 5           |
| Stearns and Friedman (1972) | Austin chalk             | 0.2                 |
| Pittman (1979)              | General statement        | 1                   |
| Weber and Bakker (1981)     | South African karst zone | 1 to 2              |
| Van Golf-Racht (1982)       | General                  | 0.001 to 3          |
| Chilingarian and Yen (1986) | General                  | 0.5 to 1.5 up to 5  |
| Bergosh and Lord (1987)     | CT scan examples         | 1.53 to 2.57        |
|                             | Epoxy injection examples | 1.81 to 9.64        |
| Confidential study          | Monterey                 | 0.01 to 1.1         |

**Table 3. Example of a Fractured Carbonate Formation  
Cementation exponent,  $m = 1.85$  Saturation exponent,  $n = 1.57$  BVWI = 4.5**

| No | POROSITY | RESISTIVITY | F     | Tau  | v    | FII  | PHIma | PHIfrc | Storativity | K    |
|----|----------|-------------|-------|------|------|------|-------|--------|-------------|------|
| 1  | 0.09     | 17.00       | 86.03 | 7.74 | 0.13 | 0.01 | 0.08  | 0.01   | 0.12        | 10   |
| 2  | 0.12     | 10.00       | 50.53 | 6.08 | 0.16 | 0.02 | 0.10  | 0.02   | 0.15        | 31   |
| 3  | 0.15     | 6.50        | 33.44 | 5.02 | 0.20 | 0.03 | 0.12  | 0.03   | 0.17        | 78   |
| 4  | 0.20     | 5.00        | 19.64 | 3.93 | 0.25 | 0.05 | 0.16  | 0.04   | 0.21        | 268  |
| 5  | 0.23     | 3.00        | 15.16 | 3.49 | 0.29 | 0.07 | 0.18  | 0.05   | 0.24        | 495  |
| 6  | 0.28     | 2.10        | 10.54 | 2.95 | 0.34 | 0.09 | 0.20  | 0.08   | 0.27        | 1207 |
| 7  | 0.28     | 4.00        | 10.54 | 2.95 | 0.34 | 0.09 | 0.20  | 0.08   | 0.27        | 1207 |
| 8  | 0.30     | 7.00        | 9.28  | 2.78 | 0.36 | 0.11 | 0.22  | 0.08   | 0.28        | 1665 |
| 9  | 0.34     | 12.00       | 7.36  | 2.50 | 0.40 | 0.14 | 0.24  | 0.10   | 0.31        | 3033 |
| 10 | 0.32     | 20.00       | 8.23  | 2.63 | 0.38 | 0.12 | 0.23  | 0.09   | 0.29        | 2263 |
| 11 | 0.25     | 15.00       | 13.00 | 3.25 | 0.31 | 0.08 | 0.19  | 0.06   | 0.25        | 719  |
| 12 | 0.26     | 10.00       | 12.09 | 3.14 | 0.32 | 0.08 | 0.19  | 0.07   | 0.26        | 859  |
| 13 | 0.27     | 20.00       | 11.27 | 3.04 | 0.33 | 0.09 | 0.20  | 0.07   | 0.26        | 1021 |
| 14 | 0.20     | 20.00       | 19.64 | 3.93 | 0.25 | 0.05 | 0.16  | 0.04   | 0.21        | 268  |
| 15 | 0.17     | 20.00       | 26.53 | 4.51 | 0.22 | 0.04 | 0.14  | 0.03   | 0.19        | 133  |
| 16 | 0.15     | 25.00       | 33.44 | 5.02 | 0.20 | 0.03 | 0.12  | 0.03   | 0.17        | 78   |
| 17 | 0.10     | 30.00       | 70.79 | 7.08 | 0.14 | 0.01 | 0.09  | 0.01   | 0.13        | 15   |
| 18 | 0.10     | 47.00       | 70.79 | 7.08 | 0.14 | 0.01 | 0.09  | 0.01   | 0.13        | 15   |
| 19 | 0.15     | 42.00       | 33.44 | 5.02 | 0.20 | 0.03 | 0.12  | 0.03   | 0.17        | 78   |
| 20 | 0.20     | 39.00       | 19.64 | 3.93 | 0.25 | 0.05 | 0.16  | 0.04   | 0.21        | 268  |
| 21 | 0.30     | 35.00       | 9.28  | 2.78 | 0.36 | 0.11 | 0.22  | 0.08   | 0.28        | 1665 |

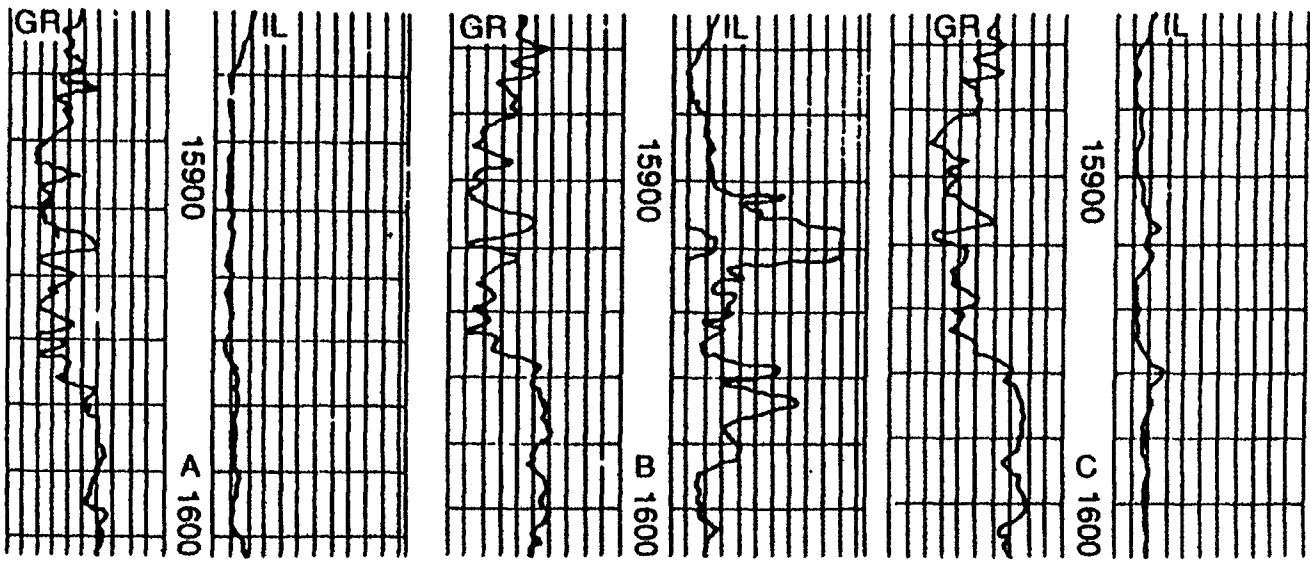


Fig. 1 Example of resistivity logs in fractured formation (Gulf Coast Well).<sup>3</sup>

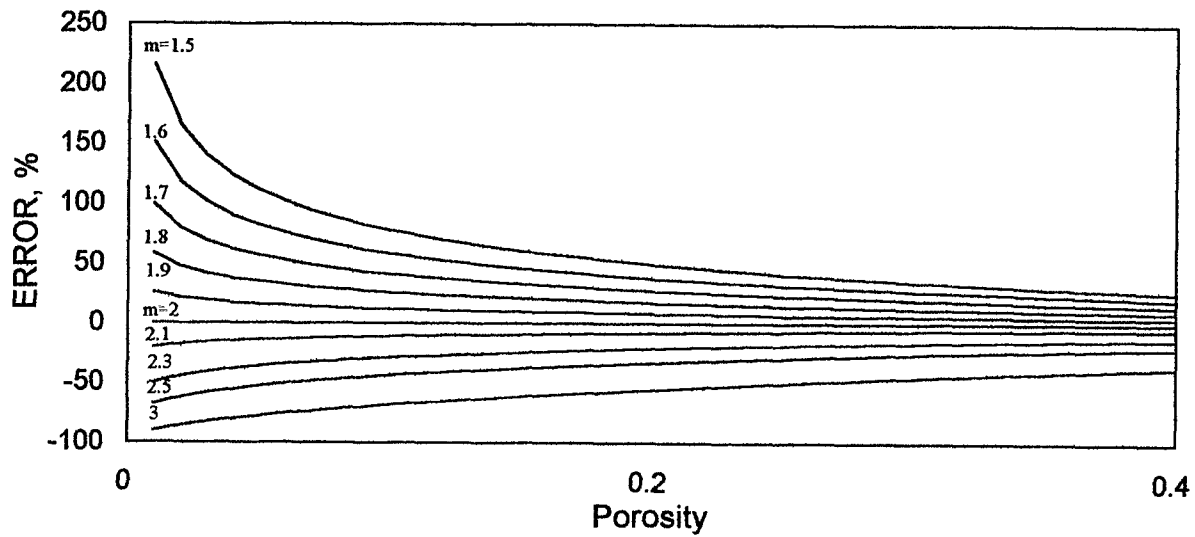


Fig. 2 Errors in reserve estimate due to incorrect  $m$  value.

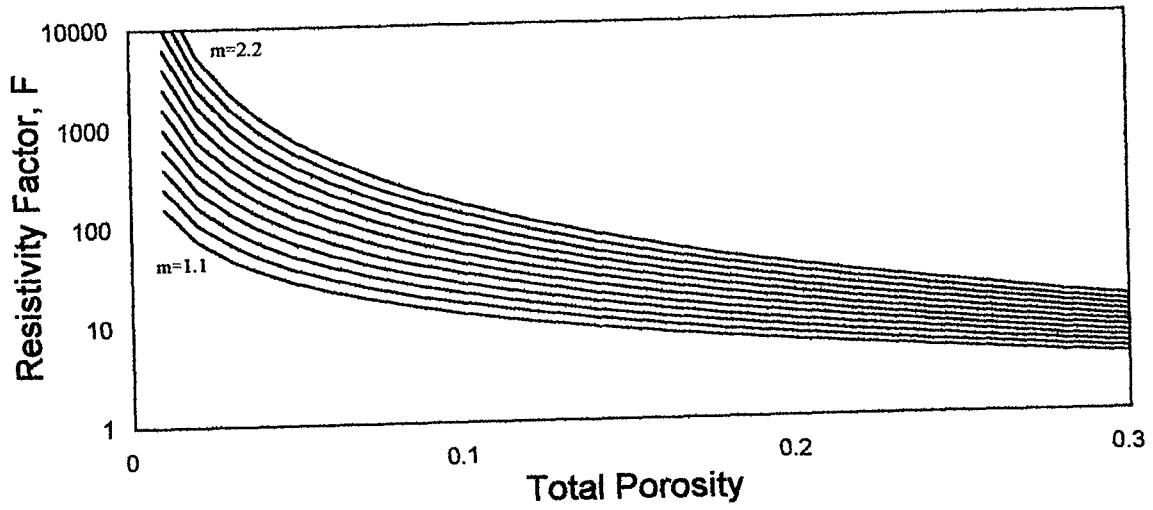


Fig. 3 A composite chart to determine fractured formation resistivity factor.

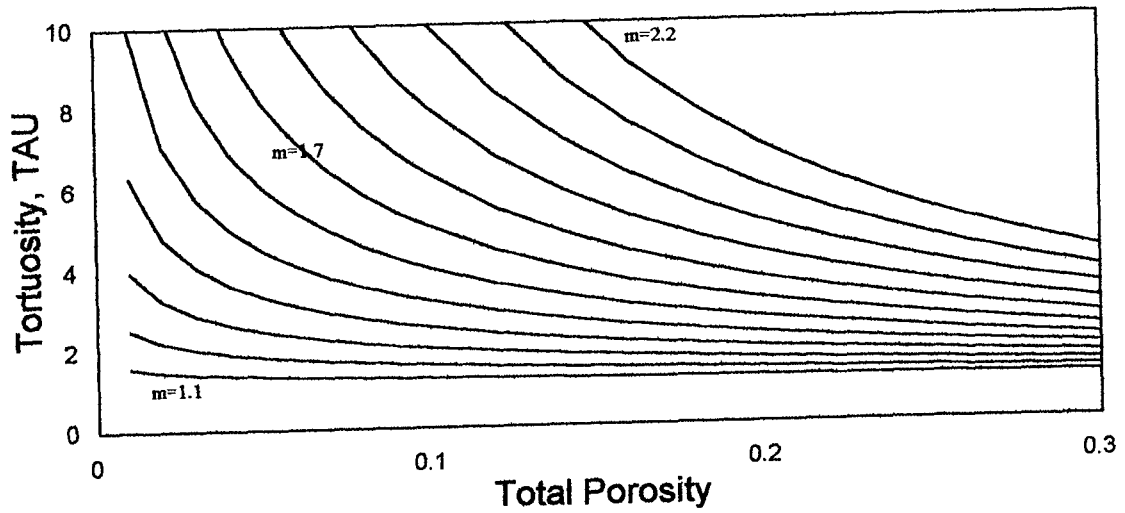


Fig. 4 A composite chart to determine fractured formation tortuosity.

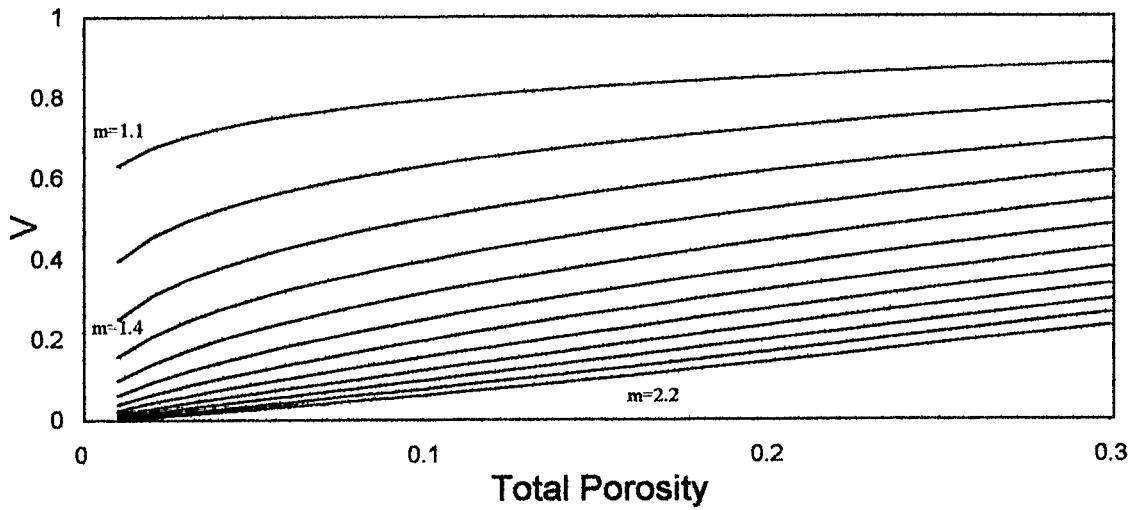


Fig. 5 A composite chart to determine partitioning coefficient,  $v$ .

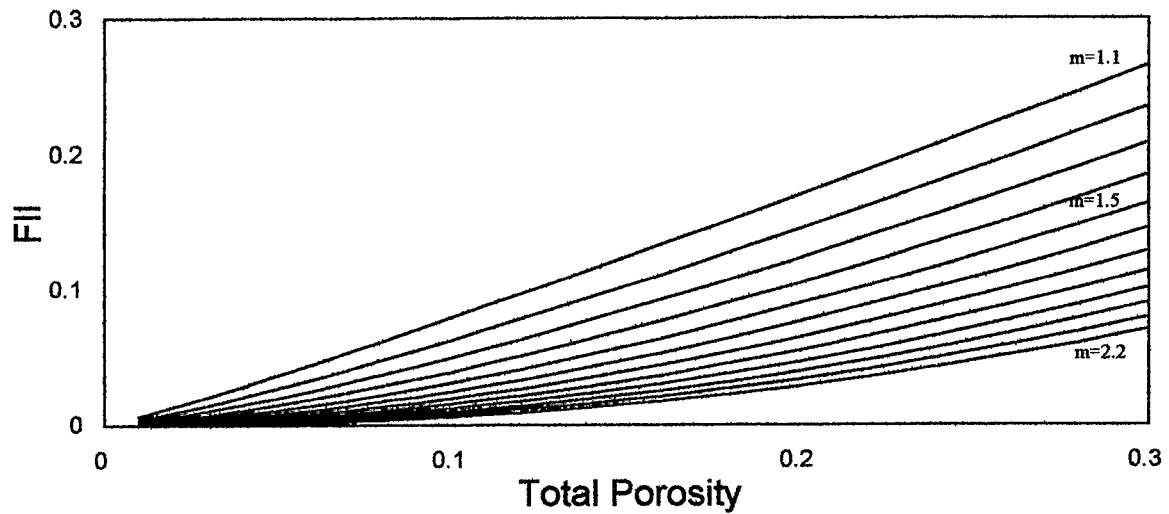


Fig. 6 A composite chart to determine fracture intensity index,  $FII$ .

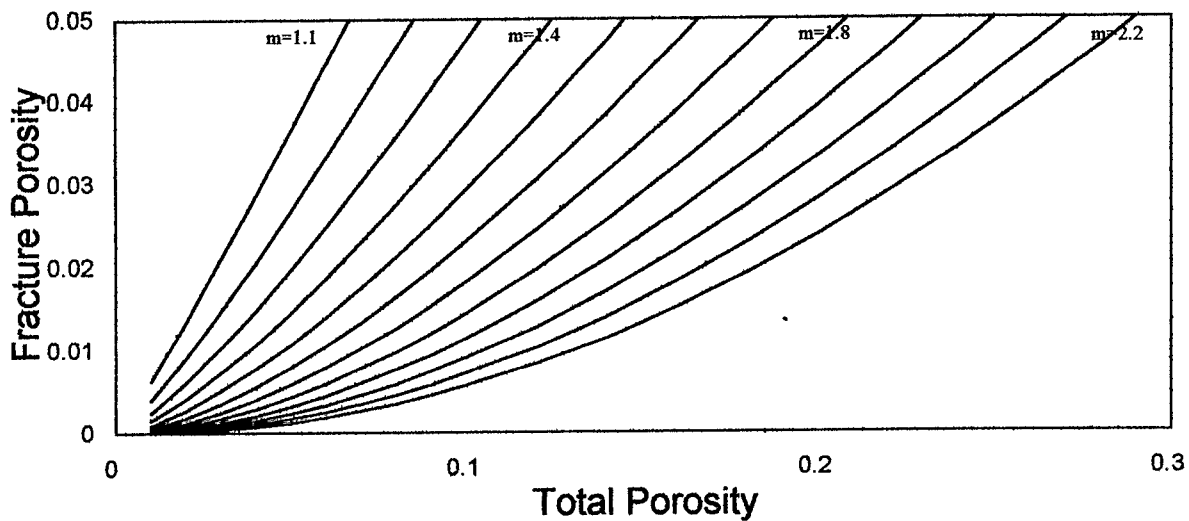


Fig. 7 A composite chart to determine fracture porosity.

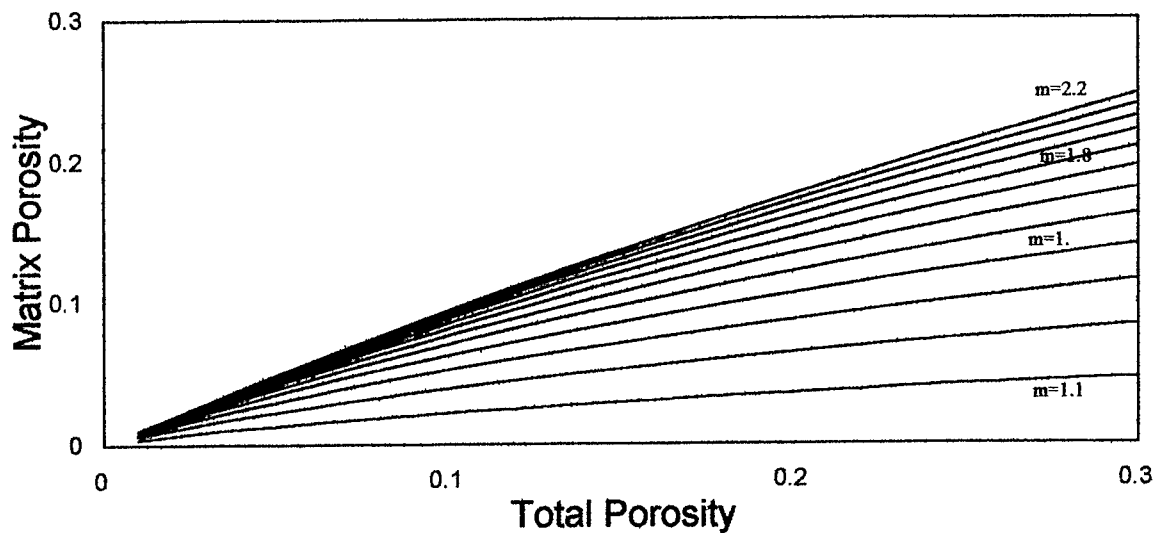


Fig. 8 A composite chart to determine matrix porosity

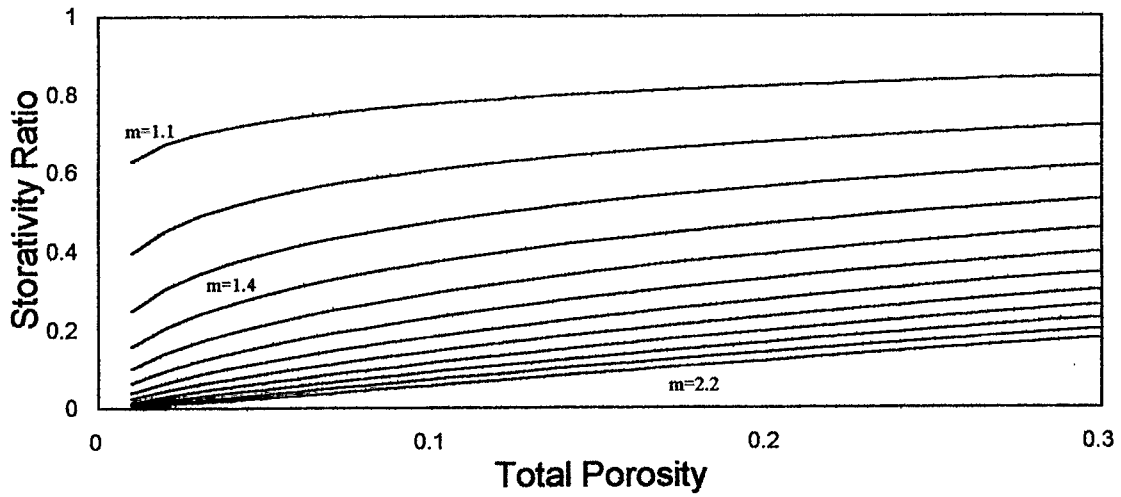


Fig. 9 A composite chart to determine fracture storativity ratio.

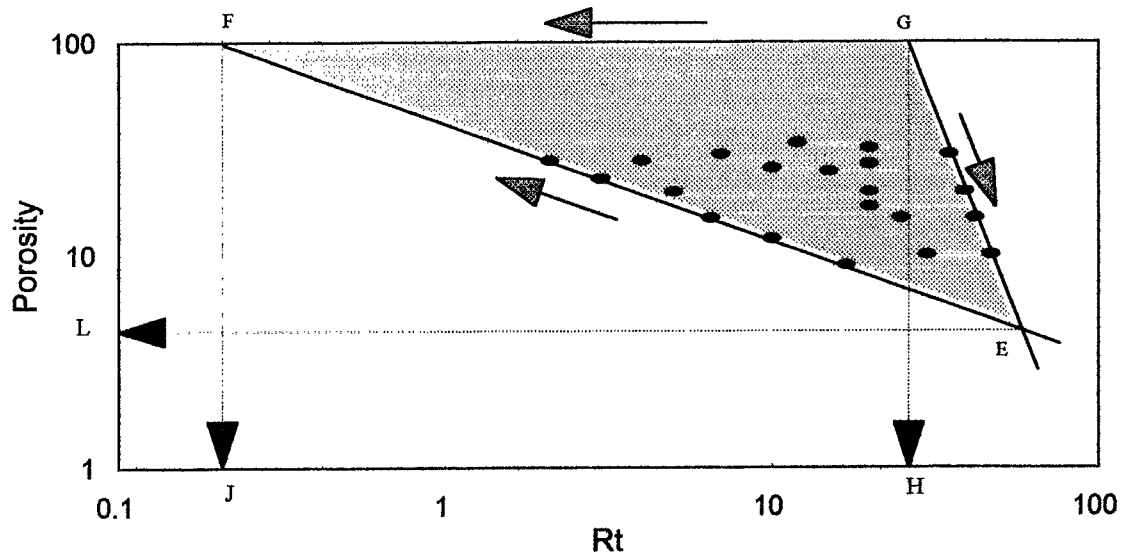


Fig. 10 Example of a fractured carbonate FM. total porosity vs. true resistivity.